

Electronic Supplementary Information

Nanozyme-like colorimetric sensing strategy based on persulfate activation on Co-based metal-organic frameworks

Zehui Deng^a, Qingling Xiao^b, Heyun Fu^a, Shourong Zheng^a, Pedro J.J. Alvarez^c,
Dongqiang Zhu^d, Zhaoyi Xu^{*a}, and Xiaolei Qu^{*a}

^a State Key Laboratory of Pollution Control and Resource Reuse, School of the Environment, Nanjing University, Nanjing 210046, China

^b Jiangsu Province Hospital on Integration of Chinese and West Medicine, Nanjing 210028, China

^c Department of Civil and Environmental Engineering, Rice University, Houston, TX 77005, United States

^d College of Urban and Environmental Sciences, Peking University, Beijing 100871, China

* Corresponding author Zhaoyi Xu, email: zhaoyixu@nju.edu.cn; Xiaolei Qu, email:

xiaoleiqu@nju.edu.cn

This file includes a total of 30 pages (including this page) with 14 figures and 2 tables.

Table of Contents

Experimental Section.....	S4
Chemicals and materials.....	S4
The synthesis of Co(BDC)TED _{0.5} and other Co-based materials.....	S5
The characterization of materials.....	S6
Catalytic PMS activation on Co(BDC)TED _{0.5} , Co(NO ₃) ₂ and other Co based catalysts.....	S6
Steady-state kinetics of PMS activation on Co(BDC)TED _{0.5}	S7
Free radical detection.....	S7
Detection of GSH by PMS activation on Co(BDC)TED _{0.5} @24h.....	S8
Calculation of the limit of detection (LOD) and limit of quantification (LOQ)....	S8
Sample collection and processing.....	S8
Fabrication of paper strip sensor.....	S9
Ethics statement.....	S9
Supplementary Discussion.....	S10
Optimization of nanozyme-like colorimetric sensor.....	S10
The calculation of turn over number (TON, K_{cat}) of Co(BDC)TED _{0.5} @24h.....	S11
Supplementary Figures	S12
Fig. S1.....	S12
Fig. S2.....	S13
Fig. S3.....	S14
Fig. S4.....	S15
Fig. S5.....	S16
Fig. S6.....	S17
Fig. S7.....	S18
Fig. S8.....	S19

Fig. S9.....	S20
Fig. S10.....	S21
Fig. S11.....	S22
Fig. S12.....	S23
Fig. S13.....	S24
Fig. S14.....	S25
Supplementary Tables.....	S26
Table S1.....	S26
Table S2.....	S27
Supplementary References.....	S28

Experimental Section

Chemicals and materials

Cobalt nitrate hexahydrate ($\text{Co}(\text{NO}_3)_2 \cdot 6\text{H}_2\text{O}$) (99%), glutathione (GSH) (98%) and terephthalic acid (H_2BDC) (98%) were obtained from Shanghai Aladdin Biochemical Technology Co. Ltd. (Shanghai, China). Potassium peroxymonosulfate ($\text{KHSO}_5 \cdot 0.5\text{KHSO}_4 \cdot 0.5\text{K}_2\text{SO}_4$, PMS) (>99%), 2,2,6,6-tetramethylpiperidine (TEMP) ($\geq 99\%$) and 5,5-dimethyl-1-pyrroline-N-oxide (DMPO) were purchased from Sigma-Aldrich Shanghai Trading Co., Ltd. Triethylene diamine (TED) (98%) was obtained from Shanghai Macklin Biochemical Technology Co. Ltd. (Shanghai, China). 3,3',5,5'-tetramethylbenzidine (TMB) was purchased from Shanghai D&B Biological Science and Technology Co. Ltd, China. Sodium acetate anhydrous, acetic acid, dimethyl sulfoxide (DMSO), tert-butyl alcohol, sodium chloride (NaCl), potassium chloride (KCl), disodium hydrogen phosphate dodecahydrate ($\text{Na}_2\text{HPO}_4 \cdot 12\text{H}_2\text{O}$), potassium dihydrogen phosphate (KH_2PO_4) and ethanol were provided by Sinopharma Chemical Reagent Co. Ltd. (Shanghai, China). Methanol was purchased from Shanghai Titan Scientific Co. Ltd. (Shanghai, China). L-Cysteine (Cys) and L-Homocysteine (Hcy), L-Alanine (Ala), L-Arginine (Arg), L-Asparagine (Asp), L-Glutamic (Glu), L-Phenylalanine (Phe), L-Methionine (Met), L-Glycine (Gly), L-Glutamine (Gln), L-Lysine (Lys), L-Tyrosine (Tyr), L-Proline (Pro), L-Serine (Ser), L-Valine (Val), L-Histidine (His), L-Isoleucine (Ile) and L-Tryptophan (Trp) were purchased from Shanghai Yuanye Biological Technology Co. Ltd. (Shanghai, China).

The synthesis of Co(BDC)TED_{0.5} and other Co-based materials

Co(BDC)TED_{0.5} with four different reaction time and other Co-based materials including Co₃O₄, Co(OH)₂ and CoFe₂O₄ were synthesized according to the references with minor modifications ¹⁻⁴.

Co(BDC)TED_{0.5}: 2 mmol Co(NO₃)₂·6H₂O in 20 ml DMF, 2 mmol H₂BDC in 30 ml DMF, and 1 mmol TED in 10 ml DMF were mixed together in a 100-mL beaker for 30 min. Then, the mixture was transferred into 100 ml Teflon-lined stainless-steel autoclave and heated at 120 °C for 6 h, 12 h, 24 h and 48 h, respectively. After naturally cooling down to room temperature, the resulting purple crystalline powder was collected via centrifugation and washed with DMF for three times and anhydrous ethanol for four times. The resulting samples were dried under vacuum at 60 °C for 12 h for further use.

Co₃O₄: 1.75 mmol of CoCl₂·4H₂O and 3.5 mmol NaCl were dissolved in 70 mL deionized water. After stirring for 30 min, 3.5 mmol of urea was added into the solution. The mixture was stirred for another hour. The resulting solution was transferred into a 100 mL Teflon-lined stainless-steel autoclave and heated at 100 °C for 12 h. After naturally cooling down to room temperature, the resulting product was collected by centrifugation and rinsed with deionized water and ethanol. The sample was dried at 80 °C overnight and calcined in air at a heating ramp of 1 °C min⁻¹ from room temperature to 300 °C and maintained at 300 °C for 3 h.

CoFe₂O₄: A 50 mL of aqueous solution containing 14.0 mmol of Co(NO₃)₂·6H₂O and 18.0 mmol of Fe(NO₃)₃·9H₂O was added into a beaker containing 100.0 mL of

NaOH solution (1 M) at 1.0 mL min^{-1} under constant stirring. The mixture was aged for 24 h at $65 \text{ }^\circ\text{C}$ under constant stirring. The dark brown CoFe_2O_4 precipitate was separated from solution by centrifugation at 5000 rpm for 5.0 min. The precipitate was washed with distilled water and then dried at $80 \text{ }^\circ\text{C}$ for 12 h.

Co(OH)_2 : 0.1 mL of ethanolamine was added to 5 mL of 0.1 M $\text{Co(CH}_3\text{COO)}_2 \cdot 4\text{H}_2\text{O}$ solution in a glass vial at room temperature. The mixture was aged at room temperature for 12 h. The pink precipitate was collected and washed several times with deionized water and ethanol. The precipitate was dried at $60 \text{ }^\circ\text{C}$ for 12 h.

The characterization of materials

Micrographs of $\text{Co(BDC)TED}_{0.5}$ were obtained by FESEM (Zeiss SUPPA™ 55, Germany). XRD measurements were conducted with $\text{Cu K}\alpha$ radiation on a D/max-Rb diffractometer (Rigaku, Japan). FT-IR spectra were collected using the KBr pellet technique on the Nicolet iS 10 infrared spectrometer (Thermo Scientific, USA). N_2 adsorption-desorption isotherms and the distribution of pore size and pore volume were measured with Micromeritics ASAP 2020 surface area and porosity analyzer (Micromeritics, USA). The absorbance of the sensor was measured using an UV-vis spectrophotometer (Shimadzu, Japan). The pH values of the reaction systems were measured using a FE20 pH meter (Mettler-Toledo Co., Germany). Free radicals were detected using an electron paramagnetic resonance (EPR) spectrometer (JES-FA200, JEOL, Japan).

Catalytic PMS activation on $\text{Co(BDC)TED}_{0.5}$, $\text{Co(NO}_3)_2$ and other Co based

catalysts

The catalytic activities of Co(BDC)TED_{0.5}, Co(NO₃)₂ and other Co-based materials were evaluated by the oxidation of colorless TMB into blue oxTMB with PMS. Acetate buffer (0.1M) was used to control the system pH at ~ 4.0⁵. The catalyst was added to the acetate buffer to form a suspension of 100 µg mL⁻¹. Then, 15 µL of the suspension was dispersed into 255 µL acetate buffer and mixed with 15 µL of PMS (1 mM in acetate buffer) and 15 µL TMB (10 mM in dimethylsulfoxide). The absorbance of the system was measured at 652 nm using a UV-vis spectrophotometer (Shimadzu, Japan) after incubating at room temperature for 8 min.

Steady-state kinetics of PMS activation on Co(BDC)TED_{0.5}

For HRP and nanozymes, the reaction kinetics can be well described by the Michaelis-Menten equation (equation 1)⁶. The values of the K_m and V_{max} are calculated by double reciprocal plot (equation 2).

$$V = V_{\max} [S] / (K_m + [S]) \quad (1)$$

$$1/v_0 = K_m/V_{\max} \cdot 1/[S] + 1/V_{\max} \quad (2)$$

Where K_m is the Michaelis constant, V_{max} is the reaction rate when the enzyme is saturated with the substrate, and [S] is the concentration of the substrate.

We performed the steady-state kinetic measurement using different concentrations of TMB (0.1, 0.2, 0.5 and 1 mM) or PMS (5, 10, 20 and 50 µM).

Free radical detection

Free radical detection was performed on an electron paramagnetic resonance (EPR) spectrometer (JES-FA200, JEOL, Japan) using DMPO and TEMP as the spin-

trapping agents. Radical scavengers were then added to the reaction system to examine the contribution of different radicals ⁷.

Detection of GSH by PMS activation on Co(BDC)TED_{0.5}@24h

The GSH detection was carried out by adding GSH with different concentrations (0-50 μ M) into the reaction system (containing Co(BDC)TED_{0.5}@24h, TMB and PMS) under the optimal conditions. The response of the sensor to other amino acids (Cys, Hcy, Ala, Arg, Asp, Glu, Phe, Met (masked by Zn²⁺), Gly, Gln, Lys, Tyr, Pro, Ser, Val, His, Ile, Trp) were examined with 50 μ M of these amino acids.

Calculation of the limit of detection (LOD) and limit of quantification (LOQ)

The limit of detection (LOD) and limit of quantification (LOQ) were calculated according to equations 3 and 4 ⁷:

$$\text{LOD} = 3S_B/k \quad (3)$$

$$\text{LOQ} = 10S_B/k \quad (4)$$

Where S_B is the standard deviation of three repeated measurements of the blank samples, and k is the slope of the regression equation when the substance is in the low concentration range.

Sample collection and processing

Three human serum samples were provided by Jiangsu Province Hospital on Integration of Chinese and West Medicine. The serum samples were stored in brown glass bottles at -18 °C after filtering through 0.45- μ m membranes to remove the proteins. Prior to detection on the colorimetric sensor, the sample is diluted 150 folds with PBS buffer. Three human serum samples and respective spiked samples (spiked

concentrations: 1 μM , 2 μM , 5 μM and 10 μM) were tested using the sensor. The comparison between spike concentration and detected concentration as well as the recoveries were used to evaluate the reliability of the sensor.

Fabrication of paper strip sensor

To make the colorimetric sensor more convenient for rapid GSH detection in human serum samples, we used the Axiva ashless filter paper (420 R, 5 μm) to prepare paper strip sensors. The filter paper strips were soaked in the standard reaction system (2 mL system volume, 500 μM TMB, 100 μM PMS and 10 $\mu\text{g mL}^{-1}$ Co(BDC)TED_{0.5}@24h) for 30 min. They were then dried at room temperature for 10 minutes. GSH solution (0.02 mM to 10 mM, 2 μL) was added to the paper strip for testing.

Ethics statement

This study was performed with the approval of the Ethics Committee for Clinical Research of Jiangsu Province Hospital on Integration of Chinese and West Medicine (2022-YJKY-029). All human serums were treated as the guidelines of the Ethics Committee for Clinical Research of Jiangsu Province Hospital on Integration of Chinese and West Medicine and informed consent was obtained.

Supplementary Discussion

Optimization of nanozyme-like colorimetric sensor

Key parameters of the sensor, such as the concentrations of Co(BDC)TED_{0.5}@24h and TMB in the system, pH, temperature and reaction time were optimized to achieve better performance.

Firstly, the concentration of Co(BDC)TED_{0.5}@24h employed in the sensor is optimized. 5 mg Co(BDC)TED_{0.5}@24h were dissolved in the 50 mL pH 4.0 acetate buffer to form a stock solution of 100 $\mu\text{g mL}^{-1}$. Different concentrations of Co(BDC)TED_{0.5}@24h varying from 1 to 10 $\mu\text{g mL}^{-1}$ were used to test the influence of Co(BDC)TED_{0.5}@24h concentration on the sensor performance. As is shown in **Fig. S11A**, as the Co(BDC)TED_{0.5}@24h concentration increases from 1 $\mu\text{g mL}^{-1}$ to 5 $\mu\text{g mL}^{-1}$, the absorbance increases from 0.2415 to 1.0599. The absorbance plateaued as the concentration of Co(BDC)TED_{0.5}@24h continues to increase. Thus, 5 $\mu\text{g mL}^{-1}$ Co(BDC)TED_{0.5}@24h was used in the sensor for GSH detection.

The influence of TMB concentration on the sensor performance was then tested. As is shown in **Fig. S11B**, as the absorbance increased from 0.4683 to 1.0529 as the TMB concentration increased from 100 μM to 500 μM , and then leveled off. Thus, 500 μM TMB was used in the sensor for GHS detection.

Acetate buffer, phosphate buffer, and ammonia buffer with pH varying from 3.0 to 10.0 were used to test the effect of solution pH on the sensor performance. As shown in **Fig. S11C**, the absorbance increased from 0.8975 to 0.9963 as the solution pH changed from 3.0 to 5.0. On the other hand, the absorbance decreased from 0.9963 to

0.3323 as the solution pH increased from 5.0 to 8.0. There is almost no color change in the reaction systems under the pH conditions of 9.0-10.0. Thus, the acetate buffer with pH ~ 5.0 was used in the sensor for GSH detection.

The reaction time and temperature were also optimized with a series of experiments (**Fig. S11D** and **Fig. S11E**). The sensor can reach the maximum absorbance of 1.0875 within 8 minutes, and the absorbance remains constant within 120 minutes. The sensor can achieve great color change effect in the temperature range of 20-70°C. These results reflect the advantages of this new sensor compared to current nanozyme sensors. The nanozyme sensor often needs 15-30 minutes to reach the maximum absorbance, and the best color effect can only be obtained under the mild condition of 35-40 °C^{5,8-10}. For the following experiments, 8 min and room temperature were selected as the most suitable reaction time and temperature for the sensor.

Overall, the conditions we used for the GSH sensor in the following experiments are summarized as follows: 5 µg mL⁻¹ Co(BDC)TED_{0.5}@24h, 500 µM TMB, 50 µM PMS, pH 5.0, and 8 min under room temperature.

The calculation of turn over number (TON, K_{cat}) of Co(BDC)TED_{0.5}@24h

K_{cat} is the turn over number, defined as the number of moles of substrate that a mole of catalyst can convert before becoming inactivated, where $K_{cat} = V_{max}/[E]$ ¹¹. When one Co cation of Co(BDC)TED_{0.5}@24h acts as the active center, $[E]=1.15\times 10^{-5}$ M, K_{cat} is calculated to be 0.026 s⁻¹ for TMB.

Supplementary Figures

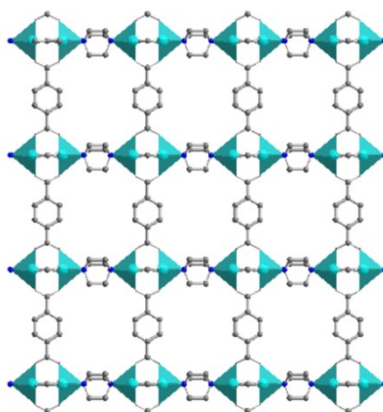


Fig. S1 The crystal structure of $\text{Co}(\text{BDC})(\text{TED})_{0.5}$. The view is along the a-axis in both cases. For clarity, solvent molecules and hydrogen molecules are omitted. Color scheme: Co (light blue); O (red); N (dark blue); C (light gray)¹².

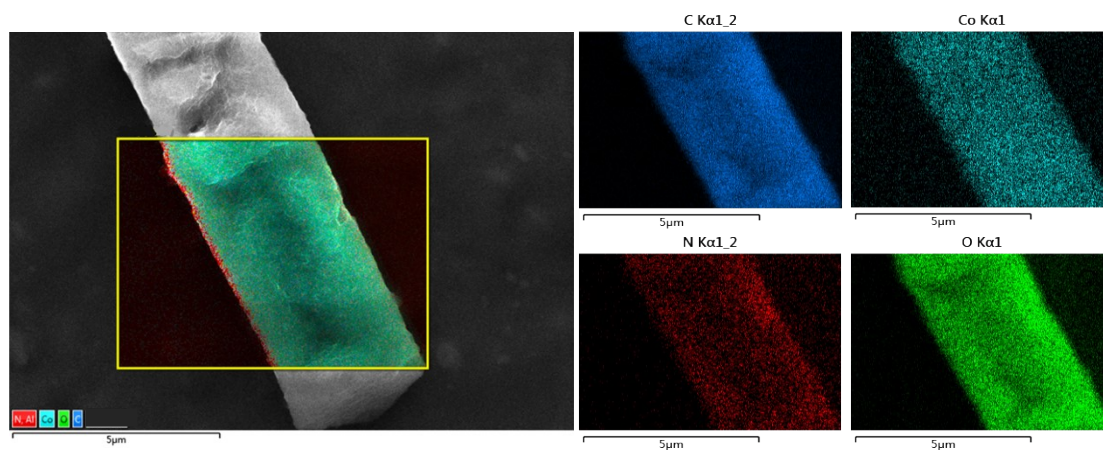


Fig. S2 Elemental mapping images for C, N, Co, O of $\text{Co(BDC)TED}_{0.5}@24\text{h}$ ($\times 10,000$) by field-emission scanning electron microscopy (FESEM).

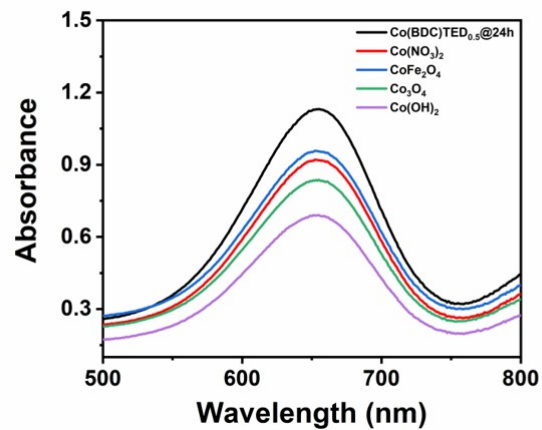


Fig. S3 UV-vis absorption spectra of systems containing different Co-based materials including Co(BDC)TED_{0.5}@24h, Co(NO₃)₂, CoFe₂O₄, Co₃O₄, and Co(OH)₂ in pH 4.0 acetate buffer.

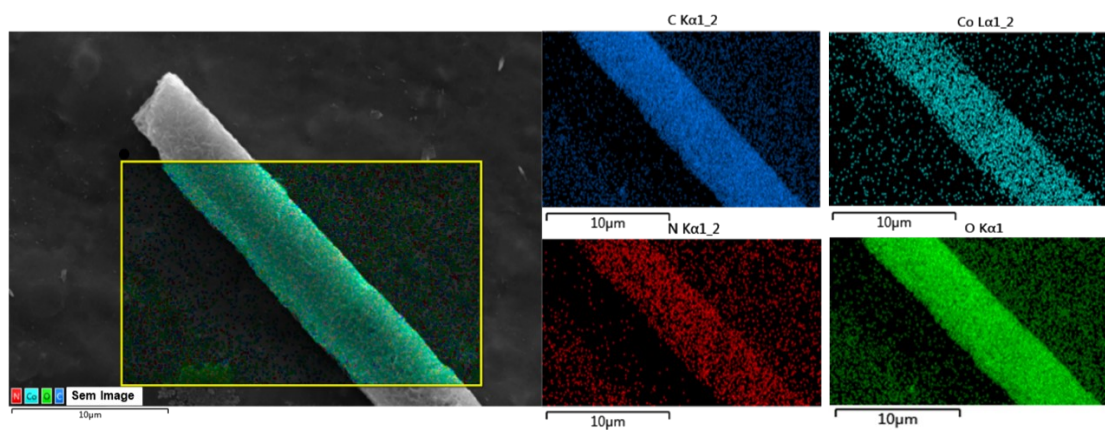


Fig.S4 Elemental mapping images for C, N, Co, O of Co(BDC)TED_{0.5}@24h ($\times 10,000$) after the colorimetric sensing by FESEM.

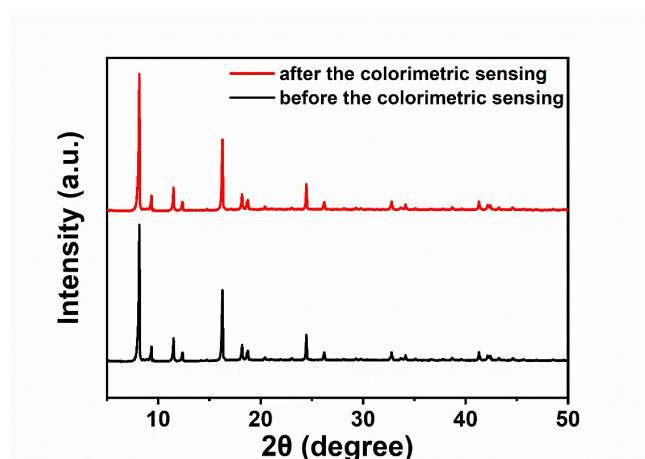


Fig. S5 PXRD profiles of Co(BDC)TED_{0.5}@24h before and after the colorimetric sensing.

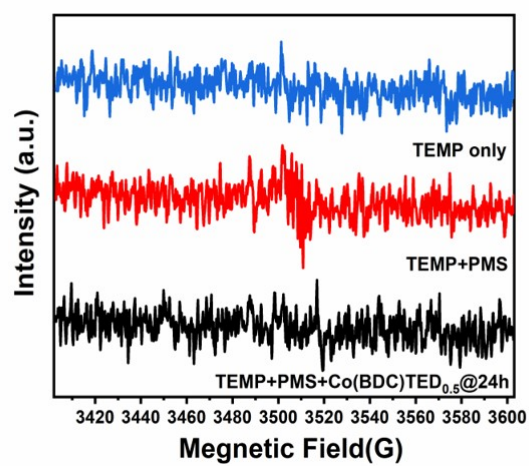


Fig. S6 EPR spectra of PMS activation on $\text{Co(BDC)TED}_{0.5}@24\text{h}$ under different conditions with 2,2,6,6-Tetramethyl-1-piperidinyloxy (TEMP).

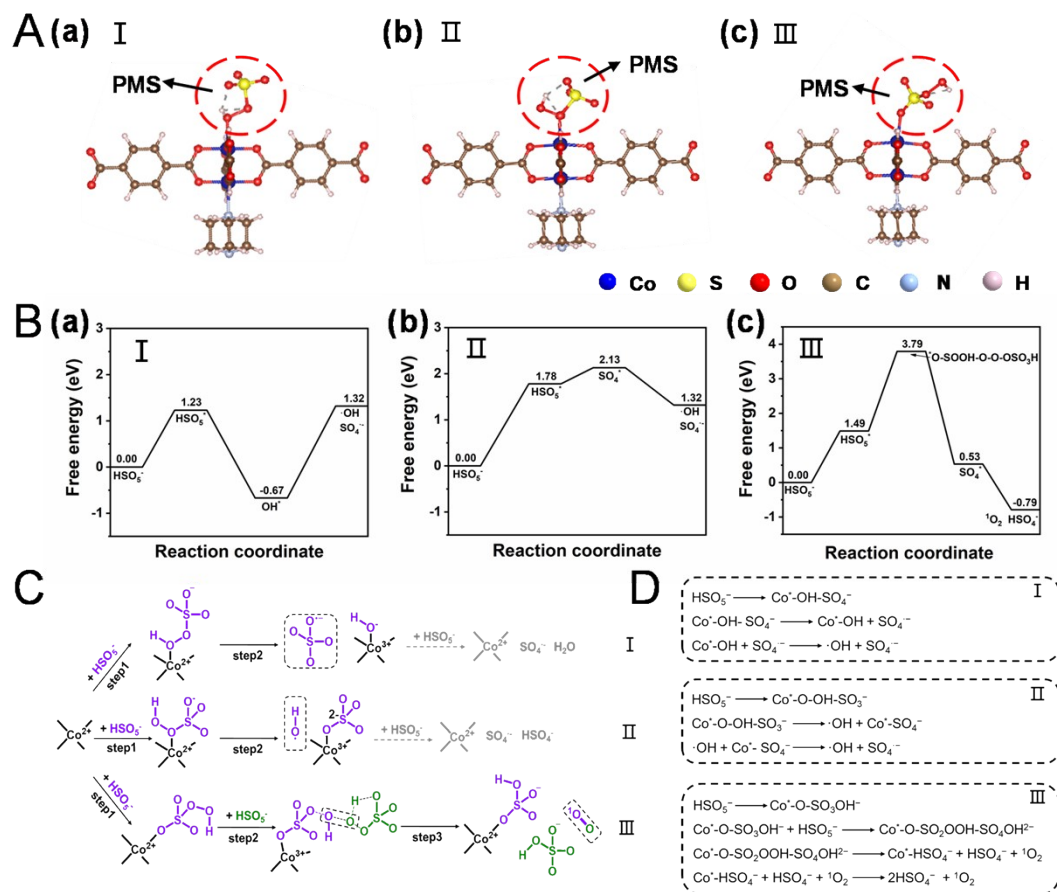


Fig. S7 The favorable pathways (I, II and III) for the adsorption and activation of PMS on Co(BDC)TED_{0.5}@24: (A) three adsorption states of PMS; (B) the energy profiles for three favorable pathways of PMS activation; (C-D) Three favorable pathways of PMS activation on Co(BDC)TED_{0.5}@24h.

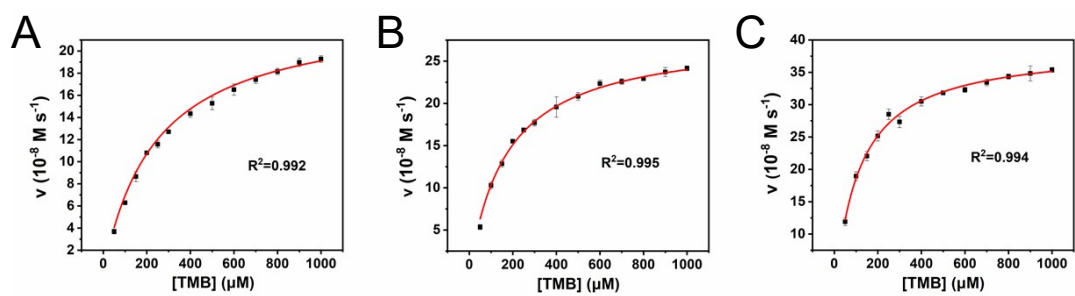


Fig. S8 Steady-state kinetics of the TMB oxidation by PMS activation on Co(BDC)TED_{0.5}@24h: Michaelis-Menten curves of Co(BDC)TED_{0.5}@24h with the concentration of PMS fixed at (A) 10 μM ; (B) 20 μM ; (C) 50 μM .

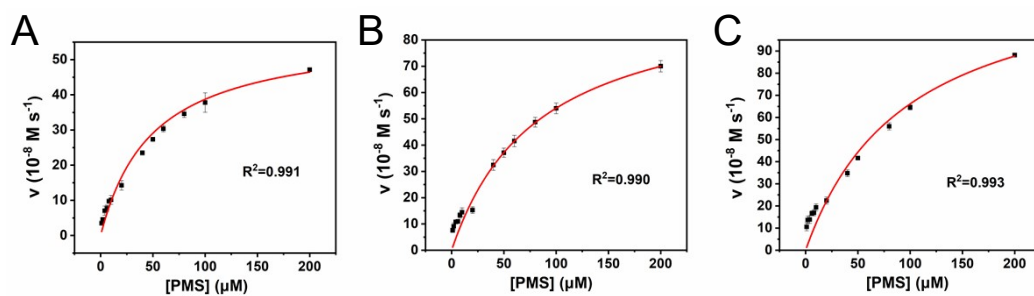


Fig. S9 Steady-state kinetics of the TMB oxidation by PMS activation on Co(BDC)TED_{0.5}@24h: Michaelis-Menten curve of Co(BDC)TED_{0.5}@24h with the concentration of TMB at (A) 100 μM ; (B) 200 μM ; (C) 500 μM .

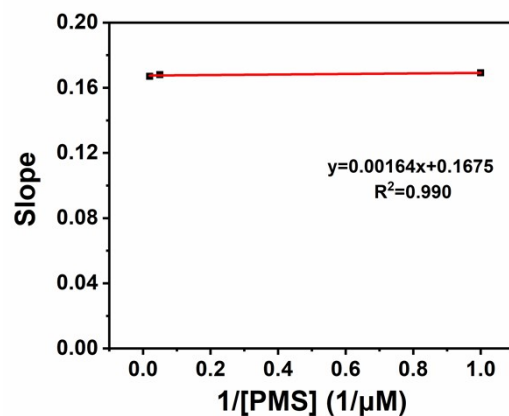


Fig. S10 Correlation between the slope values obtained in the three Lineweaver-Burk plots against inversed PMS concentration associated with Fig. 3. The linear fitting shows a very small slope (0.00164), which indicates the reaction is controlled by the ping-pong mechanism.

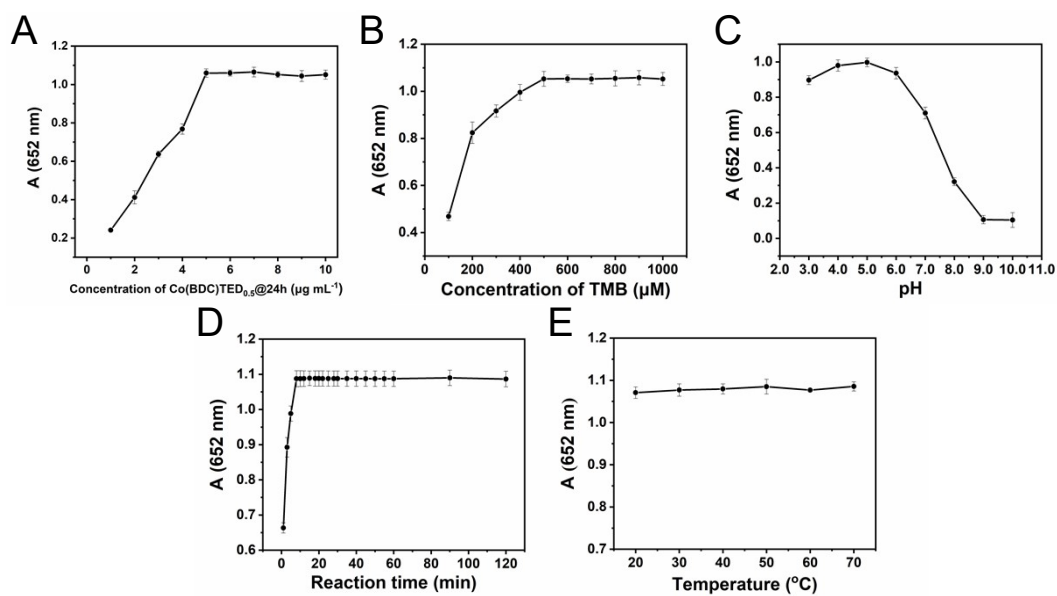


Fig. S11 Optimization of the nanozyme-like sensor: Influence of (A) the concentration of Co(BDC)TED_{0.5}@24h; (B) the concentration of TMB; (C) the pH value; (D) the reaction time; and (E) the temperature on the sensor performance.

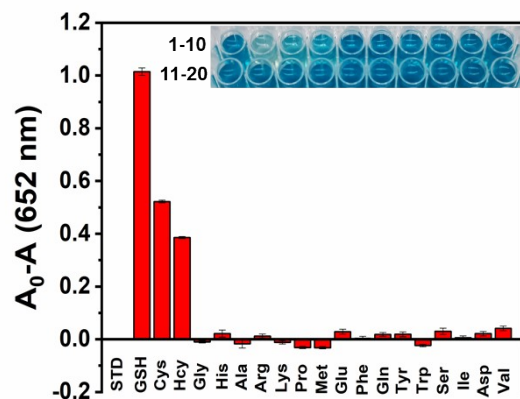


Fig. S12 Changes of the absorbance at 652 nm of the sensor with GSH (50 μ M) and other amino acids (Cys, Hcy, Ala, Arg, Asp, Glu, Phe, Met (masked by Zn^{2+}), Gly, Gln, Lys, Tyr, Pro, Ser, Val, His, Ile, Trp, 50 μ M). Inset: the corresponding photograph of sensors with amino acids. Standard solution, GSH and the other amino acids mentioned above are numbered 1-20 respectively. All measurements were carried out at room temperature for 8 min in 0.1 M acetate buffer solution at pH 5.0.

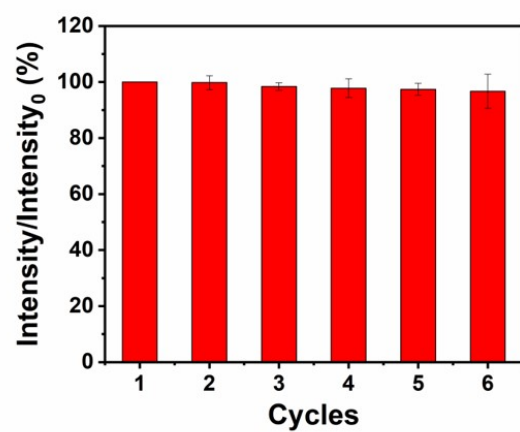


Fig. S13 The catalytic performance of Co(BDC)TED_{0.5}@24h after reuse. Reaction condition: 1 mg mL⁻¹ Co(BDC)TED_{0.5}@24h, 500 μM TMB, 500 μM PMS, pH 5.0, 8 min, under room temperature in 5 mL reaction system.

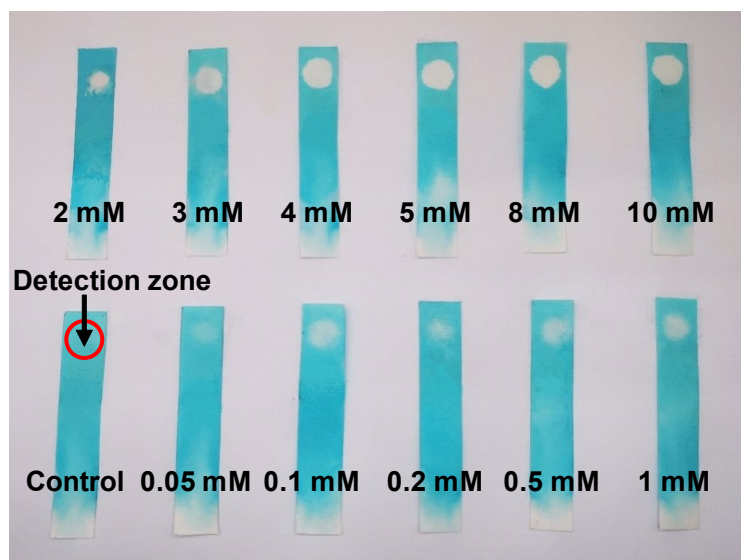


Fig. S14 Photographs of paper strip sensors after the addition of 2 μL GSH solution at the detection zone.

Supplementary Tables

Table S1 Comparisons of nanozyme-based colorimetric methods for GSH detection.

Materials	Detection time (min)	Detection pH	Detection temperature (°C)	Linear range (μM)	LOD (μM)	Reference
Commercial DTNB colorimetric Assay Kit ^a	20	-	37	40.7-650.8	40.7	-
MoS ₂ /N-rGO ^b	30	3.6	25	2-15	0.12	13
HBF-1-C800 ^c	20	3.8	-	20-1000	11.2	14
Cu-CuFe ₂ O ₄	-	4.0	35	2.5-10	0.31	15
Fe ₃ O ₄	10	4.0	45	3-30	3.0	16
Cu _{1.8} S	-	4.0	-	500-10000	60.0	17
Carbon nanodots	15	3.5	30	0-7	0.3	18
Au nanoclusters	50	4.0	30	2-25	0.42	19
PdFe/GDY ^d	-	4.0	25	10-800	4.21	20
Fe ₃ O ₄ /CNDs ^e	30	4.0	30	0.1-20	0.058	21
Co ₃ O ₄ -MMT ^f	15	4.0	40	0.1-20	0.088	22
PS MOF	25	4.0	-	0-20	0.68	23
FeMnO ₃	10	4.0	35	0-10	0.036	24
Co(BDC)TED _{0.5} @24h	8	5.0	20-70	0.1-30	0.021	This work

^a 5,5'-dithiobis-2-nitrobenoic acid;

^b MoS₂ Nanosheet/N-Doped Reduced Graphene Oxide;

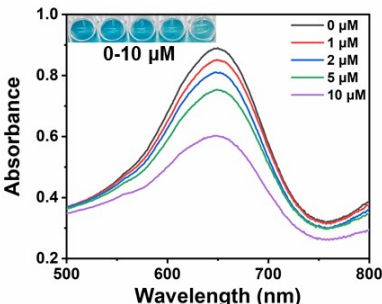
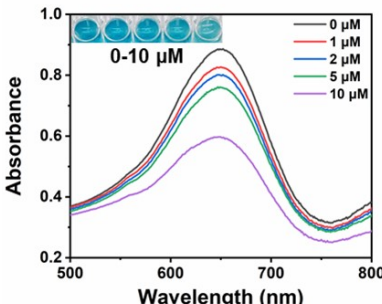
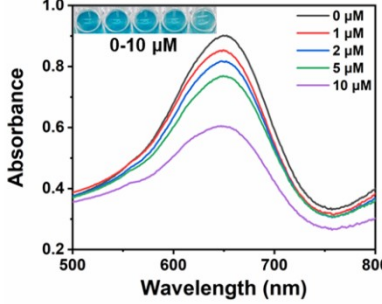
^c A hydrogen-bonded biohybrid framework (HBF) obtained from confining BSA into well-defined HOFs (hydrogen-bonded organic frameworks);

^d Palladium-iron nanostructure decorated graphdiyne nanosheet;

^e Fe₃O₄/carbon nanodots;

^f Co₃O₄ nanoparticles anchored on montmorillonite (MMT);

Table S2 GSH concentrations in three human serum samples determined by the colorimetric sensor.

Serum sample (150-folds dilution)	Added GSH (μM)	Average Detected GSH (μM)	RSD (%) (n=3)	Average recovery (%)
	0	6.328	1.752	-
	1	7.434	4.150	110.6
	2	8.293	2.203	98.3
	5	11.389	4.022	101.2
	10	16.407	3.781	100.8
	0	6.237	0.898	-
	1	7.157	5.482	92.0
	2	8.365	3.561	106.4
	5	11.371	4.117	102.7
	10	16.924	6.004	106.9
	0	5.853	2.159	-
	1	7.048	3.856	119.5
	2	8.232	1.627	119.0
	5	11.535	2.151	113.6
	10	15.236	2.067	93.8

Supplementary References

1. S. Mutahir, C. Wang, J. Song, L. Wang, W. Lei, X. Jiao, M. A. Khan, B. Zhou, Q. Zhong and Q. Hao, *Appl. Mater. Today*, 2020, **21**, 100813.
2. Q. Ren, Z. Feng, S. Mo, C. Huang, S. Li, W. Zhang, L. Chen, M. Fu, J. Wu and D. Ye, *Catal. Today*, 2019, **332**, 160-167.
3. M. Khajeh, A. R. Oveisi, A. Barkhordar and Z. Sorinezami, *Spectrochim Acta A*, 2020, **234**, 118270.
4. M. Sarif, J. Hilgert, I. Khan, R. A. Harris, S. Plana-Ruiz, M. Ashraf, E. Putz, J. Schemberg, M. Panthofer, U. Kolb, M. Nawaz Tahir and W. Tremel, *Langmuir*, 2020, **36**, 13804-13816.
5. X. Liu, L. Huang, Y. Wang, J. Sun, T. Yue, W. Zhang and J. Wang, *Sensor Actuat. B-Chem.*, 2020, **306**, 127565.
6. L. Gao, J. Zhuang, L. Nie, J. Zhang, Y. Zhang, N. Gu, T. Wang, J. Feng, D. Yang, S. Perrett and X. Yan, *Nat. Nanotechnol.*, 2007, **2**, 577-583.
7. G. X. Huang, J. Y. Si, C. Qian, W. K. Wang, S. C. Mei, C. Y. Wang and H. Q. Yu, *Anal. Chem.*, 2018, **90**, 14439-14446.
8. S. Singh, K. Mitra, A. Shukla, R. Singh, R. K. Gundampati, N. Misra, P. Maiti and B. Ray, *Anal. Chem.*, 2017, **89**, 783-791.
9. Y. Wang, Y. Sun, H. Dai, P. Ni, S. Jiang, W. Lu, Z. Li and Z. Li, *Sensor Actuat. B-Chem.*, 2016, **236**, 621-626.
10. H. Q. Zheng, C. Y. Liu, X. Y. Zeng, J. Chen, J. Lu, R. G. Lin, R. Cao, Z. J. Lin and J. W. Su, *Inorg. Chem.*, 2018, **57**, 9096-9104.

11. S. Singh, P. Tripathi, N. Kumar and S. Nara, *Biosens. Bioelectron.*, 2017, **92**, 280-286.
12. Z. Zhang, J. Liu, Z. Li and J. Li, *Dalton Trans.*, 2012, 41, 4232-4238.
13. L. Wang, B. Li, Z. You, A. Wang, X. Chen, G. Song, L. Yang, D. Chen, X. Yu, J. Liu and C. Chen, *Anal. Chem.*, 2021, **93**, 11123-11132.
14. N. Ye, S. Huang, H. Yang, T. Wu, L. Tong, F. Zhu, G. Chen and G. Ouyang, *Anal. Chem.*, 2021, **93**, 13981-13989.
15. F. Xia, Q. Shi and Z. Nan, *Dalton T.*, 2020, **49**, 12780-12792.
16. Y. Ma, Z. Zhang, C. Ren, G. Liu and X. Chen, *Analyst*, 2012, **137**, 485-489.
17. H. Zou, T. Yang, J. Lan and C. Huang, *Anal. Methods-UK*, 2017, **9**, 841-846.
18. M. Shamsipur, A. Safavi and Z. Mohammadpour, *Sensor Actuat. B-Chem.*, 2014, **199**, 463-469.
19. J. Feng, P. Huang, S. Shi, K. Y. Deng and F. Y. Wu, *Anal. Chim. Acta*, 2017, **967**, 64-69.
20. T. Wang, Q. Bai, Z. Zhu, H. Xiao, F. Jiang, F. Du, W. W. Yu, M. Liu and N. Sui, *Chem. Eng. J.*, 2021, **413**, 127537.
21. N. Luo, Z. Yang, F. Tang, D. Wang, M. Feng, X. Liao and X. Yang, *ACS Appl. Nano Mater.*, 2019, **2**, 3951-3959.
22. Y. Gao, K. Wu, H. Li, W. Chen, M. Fu, K. Yue, X. Zhu and Q. Liu, *Sensor Actuat. B-Chem.*, 2018, **273**, 1635-1639.
23. Y. Liu, M. Zhou, W. Cao, X. Wang, Q. Wang, S. Li and H. Wei, *Anal Chem*, 2019, **91**, 8170-8175.

24. M. Chi, S. Chen, M. Zhong, C. Wang and X. Lu, *Chem. Commun. (Camb)*, 2018, **54**, 5827-5830.